52. E. Christofferson, *Geol. Soc. Am. Bull.* **87**, 1255 (1976).
53. Seasat gravity data set [National Geophysical Data Center (NOAA), Boulder, CO, 1989].
54. J. E. Case and T. L. Holcombe, *U.S. Geol. Surv. Misc. Invest. Ser. Map I-1100* (1980).
55. R. A. F. Grieve and J. Alexopoulus, *Can. J. Earth Sci.* **25**, 1530 (1988).
56. V. L. Sharpton, B. C. Schuraytz, A. V. Murali, G. Ryder, K. Burke, *Global Catastrophies in Earth History: An Interdisciplinary Conference on Impacts, Volcanism, and Mass Mortality* (Lunar and Planetary Institute, Houston, 1988), pp. 172–173 (abstr.).
57. M. R. Owen and M. H. Anders, *Nature* **334**, 145 (1988).
58. R. A. Coish, *Contrib. Mineral. Petrol.* **60**, 255 (1977); J. A. Karson, in *Ophiolites and Oceanic Lithosphere*, I. G. Gass, S. J. Lippard, A. W. Shelton, Eds. (Blackwell, London, 1984), pp. 131–144.
59. J. Girardeau, J-C. C. Mercier, W. Xibin, *Contrib. Mineral. Petrol.* **90**, 309 (1985).
60. E. Christofferson and M. H. Hamil, *Geology* **6**, 341 (1978).
61. G. T. Penfield and A. Camargo, *51st Annu. Meeting Soc. Explor. Geophys. Abstr.* (1981), p. 37.
62. Data are normalized to CI chondrite data of M. N. Evensen, P. J. Hamilton, F. K. Onions, *Geochim. Cosmochim. Acta* **42**, 1199 (1978).
63. We thank E. Rosencrantz for providing unpublished University of Texas seismic reflection data, and M. Giarratano and C. Brenner for providing Lamont Doherty Geological Observatory seismic reflection data and helpful discussions. We also thank F. Maurrasse for providing access to samples of the Haitian K/T boundary sections and background information to aid our field studies, and E. Rosencrantz and C. Bowland for reviewing an earlier version of the manuscript. D. Kring helped with initial investigations of the Haitian ejecta layer, assistance in the field, and many valuable comments. This work was supported by NASA Grant NAG 9-37.

19 December 1989; accepted 16 April 1990

Structural Motif of the GCN4 DNA Binding Domain Characterized by Affinity Cleaving

MARTHA G. OAKLEY AND PETER B. DERVAN*

The NH_2-terminal locations of a dimer containing the DNA binding domain of the yeast transcriptional activator GCN4 have been mapped on the binding sites 5′-CTGACTAAT-3′ and 5′-ATGACTCTT-3′. Affinity cleaving was effected by synthetic GCN4 proteins with Fe·EDTA moieties at the NH_2-terminus. Analysis of the DNA cleavage patterns for dimers of the Fe·EDTA-proteins corresponding to GCN4 residues 222 to 281 and 226 to 281 revealed that the NH_2-termini were in the major groove nine to ten base pairs apart and were symmetrically displaced four to five base pairs from the central C of the recognition site. This result is consistent with the Y-shaped scissor grip–leucine zipper model recently proposed for a class of DNA binding proteins important in the regulation of gene expression.

A CLASS OF SEQUENCE-SPECIFIC DNA binding proteins important in the regulation of gene expression has been proposed to bind DNA through a bipartite structural motif consisting of a DNA binding domain, termed the "basic region," and a dimerization domain, termed the "leucine zipper" (*1*). These proteins recognize binding sites on DNA that consist of abutted inverted repeats. An evaluation of conserved amino acids within the basic region of several sequences from plant, mammalian, and fungal proteins located at invariant distances from the leucine zipper (bZIP proteins) has led to a provisional "scissor-grip" model for DNA binding (*2*). Vinson, Sigler, and McKnight propose that two polypeptide chains join to form a Y-shaped molecule (*2*). The stem of the Y is the dimer-forming region and corresponds to a coiled pair of amphipathic α helices, 30 amino acids long (*1*). The bifurcating arms of the Y emerge from the paired α helices and begin tracking each half site in opposite directions along the major groove of the DNA (*2*). The bZIP model predicts that a rotationally symmetric dimer forms and that the NH_2-terminal extensions of the leucine zipper bend to grip around the major groove of DNA on the side opposite to their initial approach (*2*).

Although footprinting studies are consistent with symmetrical contacts in the major groove, there is little other structural data concerning the basic region of bZIP proteins bound to DNA (*2*). Neither x-ray diffraction nor two-dimensional nuclear magnetic resonance studies have been reported on this class of DNA binding proteins. Remarkably, the Y-shaped motif has been derived mostly from model building (*2*).

We report affinity cleaving studies designed to investigate the structure of the DNA binding domain of the yeast transcriptional activator GCN4, a putative basic region–leucine zipper (bZIP) protein. GCN4 is necessary for the coordinate induction of 30 to 50 proteins involved in the biosynthesis of amino acids in response to amino acid starvation (*3*). A functional dissection of GCN4 has demonstrated that the 60 amino acids at the COOH-terminus, residues 222 to 281, contain the specific DNA binding activity; however, 37 residues (245 to 281) at the COOH-terminus were shown to be insufficient for DNA binding (*4*). GCN4 exists as a dimer and the 60 residues at the COOH-terminus are sufficient for dimerization (*5*). The optimum DNA binding site for GCN4 is 5′-rrTGACTcatt-3′ (*6*). Struhl and co-workers have proposed that this pseudosymmetric site behaves as two half-sites, noting that mutation of the naturally occurring GCN4 binding site 5′-TGACTCT-3′ to the symmetric 5′-TGACTCA-3′ increases the affinity of the protein for the DNA, whereas all other mutations in this region lead to unchanged or decreased affinity. However, mutation of the TGACT bases leads to the greatest reduction in binding affinity, and mutation of the central C to G abolishes activity, implying that the protein-DNA interactions at each half site are not equal (*6*).

Incorporation of the DNA cleaving moiety, Fe·EDTA, at discrete amino acid residues within a protein allows the positions of those residues in the protein-DNA complex relative to the DNA bases to be mapped to nucleotide resolution (*7*). After chemical activation with a reducing agent such as dithiothreitol (DTT), Fe·EDTA localized at a specific DNA binding site cleaves both DNA strands, typically over four to six base

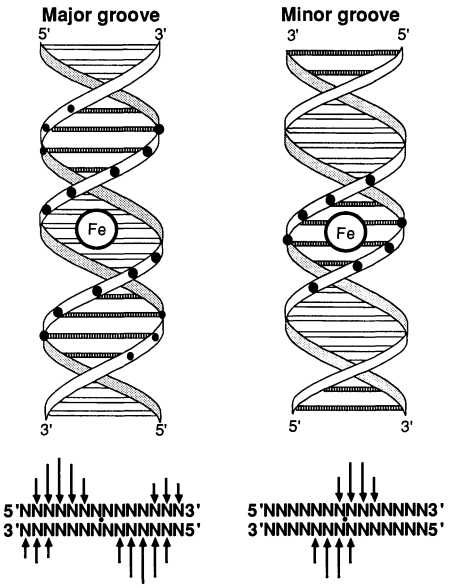

Fig. 1. Cleavage patterns produced by a diffusible oxidant generated by Fe·EDTA located in the major and minor grooves of right-handed DNA. Filled circles represent points of cleavage along the phosphodiester deoxyribose backbone. Sizes of circles represent extent of cleavage.

Arnold and Mabel Beckman Laboratories of Chemical Synthesis, Division of Chemistry and Chemical Engineering, California Institute of Technology, Pasadena, CA 91125.

*To whom correspondence should be addressed.

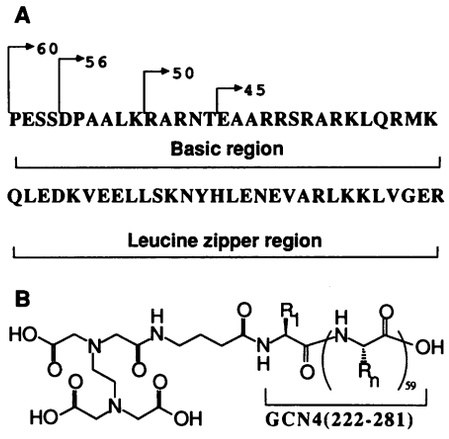

Fig. 2. (**A**) The sequence of 60 amino acids (222 to 281) corresponding to the COOH-terminus of yeast transcriptional activator GCN4 (*20*). (**B**) Synthetic protein EDTA-GCN4(222–281). Abbreviations for the amino acid residues are: A, Ala; D, Asp; E, Glu; G, Gly; H, His; I, Ile; K, Lys; L, Leu; M, Met; N, Asn; P, Pro; Q, Gln; R, Arg; S, Ser; T, Thr; V, Val; and Y, Tyr.

pairs, through a diffusible species (*8, 9*). Because of the right-handed nature of double-helical DNA, the groove in which the Fe·EDTA is located can be identified by analysis of the cleavage patterns (Fig. 1). An Fe·EDTA located in the minor groove generates an asymmetric cleavage pattern with maximal cleavage loci shifted to the 3′ side on opposite strands (*8, 9*) (Fig. 1). When the Fe·EDTA is located in the major groove, the maximal cleavage loci are 5′-shifted; in addition, cleavage of lower efficiency occurs on the distal strands of the adjacent minor grooves (*10, 11*) (Fig. 1). This results in a pair of 3′-shifted asymmetric cleavage loci of unequal intensity on opposite strands (*10, 11*) (Fig. 1). These patterns can be explained if the diffusible radical generated from the localized Fe·EDTA reacts in the major and minor grooves of DNA with unequal rates, preferentially (although not necessarily exclusively) in the minor groove (*12, 13*). The affinity cleaving method has been used to map the location of the NH_2- and COOH-termini of the DNA binding domain of Hin recombinase to the minor and major grooves, respectively (*7, 14*).

Four different proteins based on the DNA binding domain of GCN4 were synthesized by solid-phase methods (*15–17*) (Fig. 2). These proteins were incrementally shortened at the NH_2-terminus; GCN4(237–281) (45-mer), GCN4(232–281) (50-mer), GCN4(226–281) (56-mer), and GCN4-(222–281) (60-mer) were synthesized with and without EDTA attached to the NH_2-terminal residue for comparative affinity cleaving and footprinting studies of the corresponding protein-DNA complexes.

The GCN4 proteins were assayed for specific DNA binding and cleaving by analyzing the cleavage products from a restriction fragment containing both an AP1 rec-

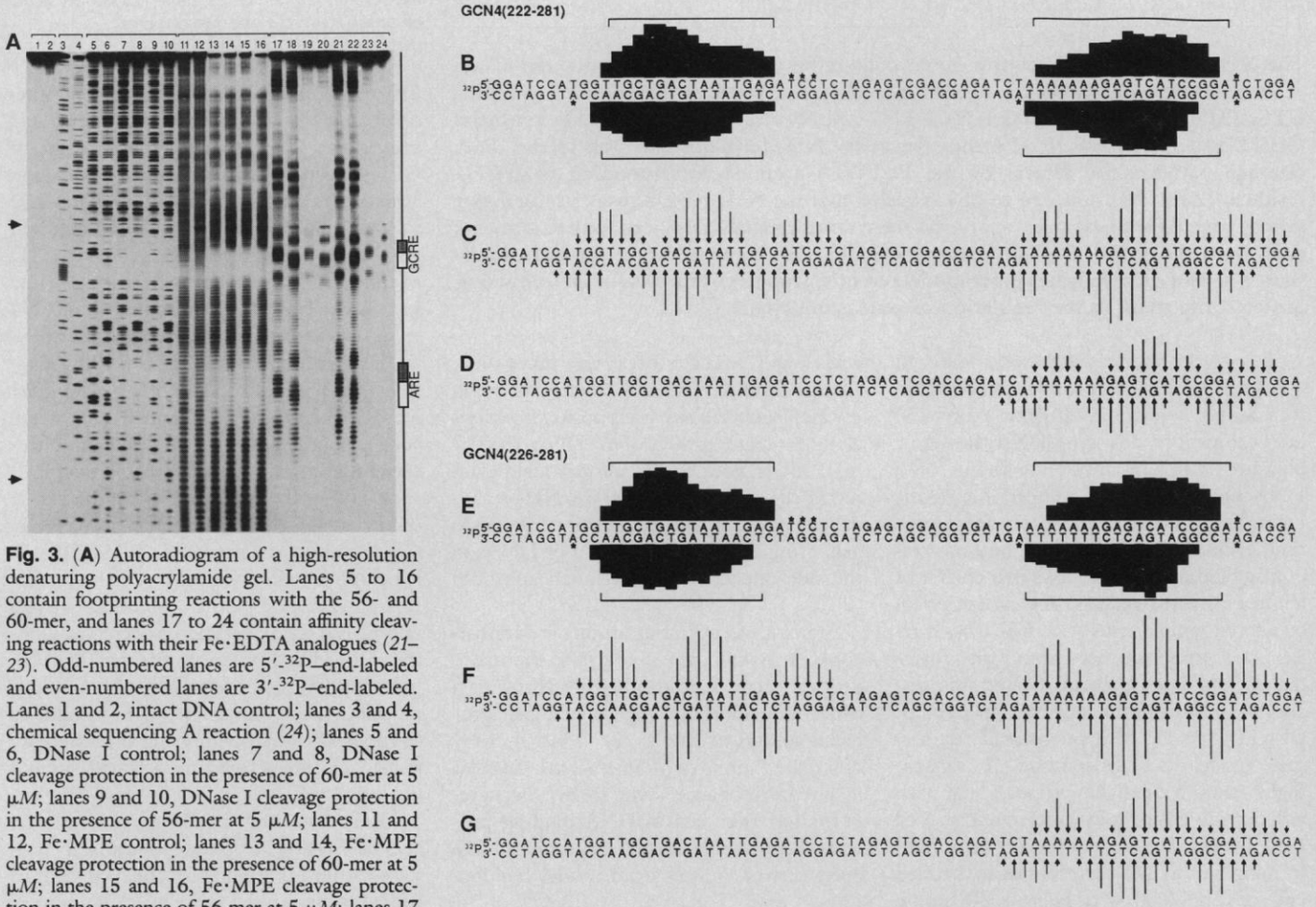

Fig. 3. (**A**) Autoradiogram of a high-resolution denaturing polyacrylamide gel. Lanes 5 to 16 contain footprinting reactions with the 56- and 60-mer, and lanes 17 to 24 contain affinity cleaving reactions with their Fe·EDTA analogues (*21–23*). Odd-numbered lanes are 5′-^{32}P–end-labeled and even-numbered lanes are 3′-^{32}P–end-labeled. Lanes 1 and 2, intact DNA control; lanes 3 and 4, chemical sequencing A reaction (*24*); lanes 5 and 6, DNase I control; lanes 7 and 8, DNase I cleavage protection in the presence of 60-mer at 5 μ*M*; lanes 9 and 10, DNase I cleavage protection in the presence of 56-mer at 5 μ*M*; lanes 11 and 12, Fe·MPE control; lanes 13 and 14, Fe·MPE cleavage protection in the presence of 60-mer at 5 μ*M*; lanes 15 and 16, Fe·MPE cleavage protection in the presence of 56-mer at 5 μ*M*; lanes 17 and 18, Fe·EDTA–60-mer at 5 μ*M*; lanes 19 and 20, Fe·EDTA–60-mer at 1 μ*M*; lanes 21 and 22, Fe·EDTA–56-mer at 5 μ*M*; and lanes 23 and 24, Fe·EDTA–56-mer at 1 μ*M*. (**B** through **G**) The sequence from left to right represents the data between the two arrows from the bottom to the middle of the gel shown on the left (A). (B) Bars represent the extent of protection from Fe·MPE cleavage in the presence of the 60-mer (A, lanes 13 and 14). Brackets represent bases protected from DNase I cleavage, and asterisks represent DNase I hypersensitivity sites (A, lanes 7 and 8). (C) Arrows represent the extent of cleavage at the indicated base position for Fe·EDTA–60-mer at 5 μ*M* (A, lanes 17 and 18). (D) Cleavage pattern for Fe·EDTA–60-mer at 1 μ*M* (A, lanes 19 and 20). (E) Fe·MPE and DNase I protection in the presence of the 56-mer at 5 μ*M* (A, lanes 9, 10, 15, and 16). (F) Cleavage pattern for Fe·EDTA–56-mer at 5 μ*M* (A, lanes 21 and 22). (G) Cleavage pattern for Fe·EDTA–56-mer at 1 μ*M* (A, lanes 23 and 24).

ognition site, 5′-CTGACTAAT-3′, and a GCN4 recognition site, 5′-ATGACTCTT-3′ (*18*). Deoxyribonuclease I (DNase I) and MPE footprinting demonstrate that the 60-, 56-, and 50-mers bind specifically to DNA at a concentration of 5 μM, whereas the 45-mer does not. The 50-, 56-, and 60-mers with Fe·EDTA also cleave DNA specifically at 5 μM concentrations. The 50-mer binds DNA with reduced affinity compared with the longer proteins. There are ten positively charged residues in the basic region extending from Lys^{231} to Lys^{251}. The 45-mer, which contains seven basic residues, is not able to bind to DNA; the 50-mer, which contains nine basic residues, binds with reduced affinity, suggesting that the missing residues are important. The 56- and 60-mers bind with approximately equal affinity.

The footprinting and affinity cleaving results for the 56- and 60-mers are shown in Fig. 3. Both proteins protect regions of ~18 base pairs at the AP1 and the GCN4 binding sites from DNase I and Fe·MPE cleavage, demonstrating sequence-specific binding (Fig. 3). The 56- and 60-mers with Fe·EDTA give cleavage patterns centered at those sites (Fig. 3). The 56- and 60-mers have greater affinity for the GCN4 site than for the AP1 site, whereas the entire GCN4 protein apparently binds to both sites with equal affinity (*18*).

Because both halves of the Fe·EDTA–56-mer and –60-mer dimers contain Fe·EDTA at the NH_2-terminus, the affinity cleavage pattern should result from the sum of two localized Fe·EDTA moieties. The cleavage pattern observed consists of three cleavage loci of unequal intensity. With regard to the cleavage model in Fig. 1, the simplest interpretation of this cleavage pattern is that it results from the superimposition of two adjacent major groove cleavage patterns along one face of the DNA (Fig. 4A). Cleavage occurs on both strands in three adjacent minor grooves, with the most efficient cleavage in the central minor groove proximal to both Fe·EDTA moieties. These data strongly suggest that the two Fe·EDTA moieties are located in adjacent major grooves. The positions of the Fe·EDTA moieties may be assigned by assuming that they lie in the center of the two 5′-shifted patterns. The Fe·EDTA moieties, and hence the NH_2-termini of the dimer, are nine to ten base pairs apart and are located four to five base pairs on either side of the central C in the binding sites 5′-CTGACTAAT-3′ and 5′-ATGACTCTT-3′ (Fig. 4). The cleavage patterns at the AP1 and GCN4 sites are similar and indicate that the protein dimer binds the two sites in much the same way.

Close scrutiny of the cleavage patterns reveals that the DNA cleavage by the Fe·EDTA–56-mer is more efficient than that by the 60-mer. This difference is especially noticeable at 1 μM concentrations, but it is found at all sites at all concentrations (Fig. 3A, lanes 19, 20, 23, and 24). As the footprinting data show that the proteins bind with roughly equal affinity, this difference in cleavage intensity may indicate that the Fe·EDTA is closer to the DNA when it is attached to Asp^{226}. One curious aspect of our data is that the Fe·EDTA moiety appears to be located in approximately the same base pair position whether it is attached to Pro^{222} or to Asp^{226}. A secondary structural element could bring these two residues in near enough proximity for the Fe·EDTA moiety to give similar cleavage patterns (*19*).

Affinity cleaving indicates that the NH_2-termini of the 60-mer dimer are (i) in the major groove of DNA, (ii) separated by nine to ten base pairs, and (iii) symmetrically displaced four to five base pairs from the central C of the recognition site (Fig. 4, B and C). This experimental result places the NH_2-termini in successive major grooves on one face of the DNA and is consistent with the proposed Y-shaped scissor-grip motif for bZIP proteins (*21*).

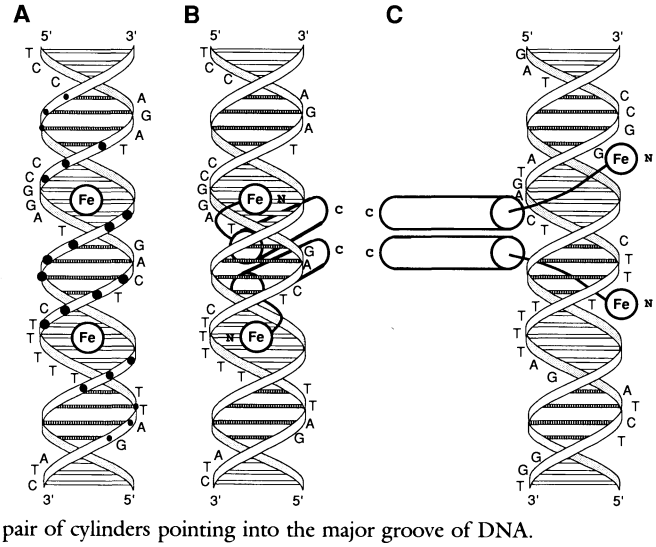

Fig. 4. (**A**) Location of the two Fe·EDTA moieties at the NH_2-termini of a 60-mer dimer assigned from the cleavage patterns for Fe·EDTA–60-mer on the GCN4 binding site, 5′-ATGACTCTT-3′. Filled circles represent the positions of cleavage along the phosphodiester deoxyribose backbone. Sizes of circles represent the extent of cleavage at the indicated base position. (**B**) Front view of a Y-shaped model for the dimer of the DNA binding domain of GCN4 with Fe·EDTA at the NH_2-termini. (**C**) Side view. The leucine zipper dimerization domains are represented by a pair of cylinders pointing into the major groove of DNA.

REFERENCES AND NOTES

1. W. H. Landschulz, P. F. Johnson, S. L. McKnight, *Science* **240**, 1759 (1988); T. Kouzarides and E. Ziff, *Nature* **336**, 646 (1988); P. Sassone-Corsi, L. J. Ransone, W. W. Lamph, I. Verma, *ibid.*, p. 692; E. K. O'Shea, R. Rutkowski, P. S. Kim, *Science* **243**, 538 (1989); W. H. Landschulz, P. F. Johnson, S. L. McKnight, *ibid.*, p. 1681; R. Turner and R. Tjian, *ibid.*, p. 1689; R. Gentz, F. J. Rauscher III, C. Abate, T. Curran, *ibid.*, p. 1695; M. Neuberg, M. Schuermann, J. B. Hunter, R. Müller, *Nature* **338**, 589 (1989); P. Agre, P. F. Johnson, S. L. McKnight, *Science* **246**, 922 (1989); P. K. Vogt, T. J. Bos, R. F. Doolittle, *Proc. Natl. Acad. Sci. U.S.A.* **84**, 3316 (1987).
2. C. R. Vinson, P. B. Sigler, S. L. McKnight, *Science* **246**, 911 (1989).
3. E. W. Jones and G. R. Fink, in *The Molecular Biology of the Yeast Saccharomyces: Metabolism and Gene Expression*, J. N. Strathern, E. W. Jones, J. R. Broach, Eds. (Cold Spring Harbor Laboratory, Cold Spring Harbor, NY, 1982), pp. 181–299.
4. I. A. Hope and K. Struhl, *Cell* **46**, 885 (1986).
5. ———, *EMBO J.* **6**, 2781 (1987).
6. D. E. Hill, I. A. Hope, J. P. Macke, K. Struhl, *Science* **234**, 451 (1986); I. A. Hope and K. Struhl, *Cell* **43**, 177 (1985).
7. J. P. Sluka, S. J. Horvath, M. F. Bruist, M. I. Simon, P. B. Dervan, *Science* **238**, 1129 (1987).
8. J. S. Taylor, P. B. Schultz, P. B. Dervan, *Tetrahedron* **40**, 457 (1984).
9. P. B. Dervan, *Science* **232**, 464 (1986).
10. H. E. Moser and P. B. Dervan, *ibid.* **238**, 645 (1987).
11. L. C. Griffin and P. B. Dervan, *ibid.* **245**, 967 (1989).
12. Several lines of evidence support this view. Tullius and Dombrowski have shown that a sinusoidal cleavage pattern is obtained when DNA is bound to a precipitate of calcium phosphate and allowed to react with Fe·EDTA, demonstrating that the two grooves have a different reactivity toward Fe·EDTA (*13*). Fe·EDTA attached to minor groove binding molecules affords cleavage patterns with single 3′-shifted asymmetric cleavage loci per Fe·EDTA position (*8, 9*). However, when Fe·EDTA is bound in the major groove of DNA by oligonucleotide triple helix formation, cleavage occurs along both strands of the adjacent minor grooves to afford a pair of cleavage loci of unequal intensity (*10, 11*). Cleavage is more intense along the strands proximal to the Fe·EDTA than along the distal strands of the adjacent minor grooves.
13. T. D. Tullius and B. A. Dombrowski, *Science* **230**, 679 (1985); *Proc. Natl. Acad. Sci. U.S.A.* **83**, 5469 (1986).
14. J. P. Sluka, S. J. Horvath, A. C. Glasgow, M. I. Simon, P. B. Dervan, *Biochemistry*, in press. D. P. Mack *et al.*, *ibid.*, in press.
15. The proteins were prepared from a single stepwise manual solid-phase peptide synthesis (*7, 14, 16*). γ-Aminobutyric acid (GABA) and EDTA, protected as the tricyclohexyl ester (*17*), were coupled to the NH_2-terminus of each protein and deprotected with anhydrous HF. Each crude protein-EDTA was purified by reverse phase high-performance liquid chromatography.
16. S. B. H. Kent, *Annu. Rev. Biochem.* **57**, 957 (1988).
17. J. H. Griffin, thesis, California Institute of Technology, Pasadena, CA (1990).
18. K. D. Harshman, W. S. Moye-Rowley, C. S. Parker, *Cell* **53**, 321 (1988).
19. Based on sequence similarity (Pro-Glu-Ser-Ser-

Asp), one candidate for this structural element would be an Ω loop. See J. F. Leszczynski and G. D. Rose, *Science* **234**, 849 (1986).
20. A. G. Hinnesbusch, *Proc. Natl. Acad. Sci. U.S.A.* **81**, 6442 (1984); G. Thireos, M. D. Penn, H. Greer, *ibid.*, p. 5096.
21. All assays were performed on a ^{32}P–end-labeled restriction fragment (Eco RI–Pvu II) from the plasmid pARE/GCRE, which contains an AP1 binding site (ARE) and a GCN4 binding site (GCRE) (boxes on right) (*18*). DNase I footprinting (*22*) reaction conditions were 10 m*M* tris·HCl, 10 m*M* KCl, 10 m*M* $MgCl_2$, 5 m*M* $CaCl_2$, 200 μ*M* dithiothreitol (DDT), 0,33 μg/ml DNase I, 200 μ*M* calf thymus DNA (bp), and 30,000-cpm end-labeled DNA, *p*H 7.0. Reactions were initiated with the addition of DNase and DTT, then allowed to proceed at room temperature for 3.5 min. The MPE footprinting (*23*) reaction conditions were 20 m*M* phosphate, 20 m*M* NaCl, 5 m*M* DTT, 5 μ*M* Fe(II)·MPE, 100 μ*M* calf thymus DNA (bp), and 30,000-cpm labeled DNA, *p*H 7.5. Reactions were initiated by the addition of DTT and Fe(II)·MPE and allowed to proceed 10 min at room temperature. Affinity cleaving reaction conditions were 30 m*M* tris·HCl, 3 m*M* sodium acetate, 20 m*M* NaCl, 5 m*M* DTT, 100 μ*M* calf thymus DNA, and 30,000-cpm labeled DNA, *p*H 7.9. After an equilibration period of 30 min, the reactions were initiated with the addition of DTT and allowed to proceed at room temperature for 30 min. Cleavage products were analyzed on an 8%, 1:20 cross-linked denaturing polyacrylamide wedge-shaped gel.
22. D. Galas and A. Schmitz, *Nucleic Acids Res.* **5**, 3157 (1978).
23. M. W. Van Dyke and P. B. Dervan, *ibid.* **11**, 5555 (1983).
24. B. L. Iverson and P. B. Dervan, *ibid.* **15**, 7823 (1987).
25. Supported by grants from the DARPA University Research Initiative Program, the National Foundation for Cancer Research, and an NSF predoctoral fellowship to M.G.O. We thank C. S. Parker for the plasmid pARE/GCRE (*18*).

16 January 1990; accepted 23 March 1990

Interaction of Hsp 70 with Newly Synthesized Proteins: Implications for Protein Folding and Assembly

RICHARD P. BECKMANN, LEE A. MIZZEN, WILLIAM J. WELCH

The 70-kilodalton family of heat shock proteins (Hsp 70) has been implicated in posttranslational protein assembly and translocation. Binding of cytosolic forms of Hsp 70 (Hsp 72,73) with nascent proteins in the normal cell was investigated and found to be transient and adenosine triphosphate (ATP)–dependent. Interaction of Hsp 72,73 with newly synthesized proteins appeared to occur cotranslationally, because nascent polypeptides released prematurely from polysomes in vivo can be isolated in a complex with Hsp 72,73. Moreover, isolation of polysomes from short-term [^{35}S]Met-labeled cells (pulsed) revealed that Hsp 72,73 associated with nascent polypeptide chains. In cells experiencing stress, newly synthesized proteins co-immunoprecipitated with Hsp 72,73; however, in contrast to normal cells, interaction with Hsp 72,73 was not transient. A model consistent with these data suggests that under normal growth conditions, cytosolic Hsp 72,73 interact transiently with nascent polypeptides to facilitate proper folding, and that metabolic stress interferes with these events.

IN MOST ORGANISMS ADVERSE changes in the local environment result in increased expression of heat shock or stress proteins (*1*). Most inducers of the stress response represent treatments that perturb protein structure and folding (*2*). The Hsp 70 family of stress proteins consists of at least four major members, all of which are related in structure and bind ATP. These include (i) constitutively expressed Hsp 73, present in cytosol and nucleus; (ii) the highly stress-inducible Hsp 72, present in cytosol, nucleus, and nucleolus; (iii) the constitutive glucose-regulated protein (Grp) 78 kD (or BiP) present in endoplasmic reticulum (ER); and (iv) the recently identified, constitutive Grp 75 kD protein present in mitochondria (*3*). Studies indicate that Hsp 70 family members interact transiently with various cellular proteins that are in the process of maturation. For example, in yeast, the cytosolic Hsp 70 proteins are essential in facilitating translocation of proteins across ER or mitochondrial membranes (*4*). Hsp 72,73 also facilitate disassembly of clathrin-coated vesicles (*5*). Finally, BiP interacts with proteins that are translocated into and assembled within the ER lumen (*6*). The interaction of the Hsp 70 family member with its target proteins is transient, with release of the target dependent on ATP hydrolysis. We present data that are consistent with the idea that most, if not all, proteins transiently interact with cytosolic Hsp 70 during their normal maturation, and we discuss how these observations relate to the stress response.

Interaction of Hsp 70 with intracellular proteins was examined by immunoprecipitation with monoclonal antibodies specific for Hsp 72,73 (Fig. 1). Duplicate plates of HeLa cells growing at 37°C were labeled with [^{35}S]Met for 20 min. One group of cells was immediately harvested (pulsed), while a second group was incubated 2 hours more without label and then harvested (pulse-chased). After cells were lysed, ATP was added to half of the lysate, while the other half was treated with apyrase to degrade endogenous ATP. In the pulse-labeled cell lysates depleted of endogenous ATP, immunoprecipitation with antibodies to Hsp 72,73 (anti-Hsp 72,73) resulted in the coprecipitation of many newly synthesized polypeptides ranging in size from 20 to 200 kD (Fig. 1B). Proteins of defined size were coprecipitated along with a background smear of labeled material, perhaps representing unfinished nascent polypeptide chains. In contrast, few proteins coprecipitated when the pulse-labeled cell lysate was incubated with exogenous ATP. Cells that were pulse-labeled with [^{35}S]Met and then incubated for 2 hours without label exhibited a different pattern of coprecipitating proteins (Fig. 1B). Specifically, fewer proteins coprecipitated with Hsp 72,73 in lysates treated with apyrase. Again, fewer proteins coprecipitated when ATP was added to the cell lysate.

We next investigated the interaction of Hsp 70 with newly synthesized proteins in HeLa cells treated with the proline analog, L-azetidine 2-carboxylic acid (Azc) to induce stress. Cells were treated with Azc for 4 hours, labeled for 15 min with [^{35}S]Met while still in the presence of the analog, and immediately harvested (pulsed) or further incubated in the absence of label and Azc for 2 hours (pulsed-chased) (Fig. 1C). Significant amounts of labeled proteins coprecipitated with anti-Hsp 72,73 in apyrase-treated lysates. Addition of ATP to immunoprecipitation yielded considerably fewer coprecipitating proteins. However, contrary to results obtained for normal (unstressed) cells (Fig. 1B), the amount of coprecipitating material was not reduced after a subsequent chase period (Fig. 1C). Instead, most of the precipitating proteins were still complexed with Hsp 72,73 after the 2-hour chase period.

We also examined the effects of no prior treatment or addition of a nonhydrolyzable ATP analog (AMPPNP) to the cell lysates prior to immunoprecipitation. In either case, an intermediate amount of newly synthesized proteins coprecipitated with Hsp 72,73. Partial release was probably due to endogenous ATP in untreated lysates. Moreover, results with AMPPNP indicate that ATP hydrolysis is required for complete release of coprecipitating proteins (*7*).

Exposure of cells to the antibiotic, puromycin, in concentrations sufficient to release nascent polypeptides from polysomes but

Departments of Medicine and Physiology, University of California, San Francisco, San Francisco, CA 94143.